7-Ketocholesterol–Induced Inflammation: Involvement of Multiple Kinase Signaling Pathways via NFκB but Independently of Reactive Oxygen Species Formation

Ignacio M. Larrayoz, Jiahn-Dar Huang, Jung Wha Lee, Iranzu Pascual, and Ignacio R. Rodríguez

Purpose. 7-Ketocholesterol (7KCh) accumulates in oxidized lipoprotein deposits and is known to be involved in macrophage foam cell formation and atherosclerosis. 7-KCh is present in the primate retina and is associated with oxidized lipoprotein deposits located in the choriocapillaris, Bruch's membrane, and retinal pigment epithelium (RPE). 7-KCh can also be formed in the retina as a consequence of light-induced iron release. The purpose of this study was to examine the signaling pathways involved in the 7KCh-mediated inflammatory response focusing on three cytokines, VEGF, IL-6, and IL-8

Methods. ARPE-19 cells were treated with 7KCh solubilized in hydroxypropyl-β-cyclodextrin. Cytokines were quantified by qRT-PCR (mRNA) and ELISA (protein) using commercially available products. NFκB activation was determined by IκBα mRNA induction

Results. Treatment of ARPE-19 cells with 15 μM 7KCh markedly induced the expression of VEGF, IL-6, and IL-8. No increase in NOX-4 expression or ROS formation was detected. 7KCh induced the phosphorylation of ERK1/2 and p38MAPK, and inhibitors to these kinases markedly reduced the cytokine expression but did not affect the IκBα mRNA expression. By contrast, inhibition of PI3K and PKCζ significantly decreased the cytokine and IκBα mRNA expression. Inhibition of the IκB kinase complex essentially ablated all cytokine induction

Conclusions. 7KCh induces cytokines via three kinase signaling pathways, AKT-PKCζ-NFκB, p38 MAPK, and ERK. The MAPK/ERK pathways seem to preferentially enhance cytokine induction downstream from NFκB activation. The results of this study suggest that 7KCh activates these pathways through interactions in the plasma membrane, but the mechanism(s) remains unknown. (*Invest Ophthalmol Vis Sci.* 2010;51:4942–4955) DOI:10.1167/iovs.09-4854

The highly toxic cholesterol oxide 7-ketocholesterol (7KCh) is found in atherosclerotic plaques.[1–7] This oxysterol is suspected of causing foam cell transformation in macrophages and toxicity to vascular endothelial and smooth muscle cells.[1–7] In the primate retina, 7KCh has been found associated with lipoprotein deposits in Bruch's membrane, choriocapillaris, and RPE cells.[8] 7-KCh is formed nonenzymatically by two known mechanisms, singlet oxygen, which requires a photosensitizing agent,[9,10] and free radical, which requires a transition metal catalyst, most commonly copper or iron.[11] In lipoprotein deposits[12,13] and in the retina,[14] the free radical mechanism, also known as the Fenton reaction, is the predominant process by which 7KCh is formed.

One of the most important consequences of 7KCh formation and accumulation are its proinflammatory properties.[1,3,5,7] 7-KCh is known to induce vascular endothelial growth factor (VEGF),[8,15] interleukin-1β,[16] interleukin (IL)-6,[17,18] and IL-8.[8,19–22] Similar properties have been reported for oxidized low-density lipoprotein (oxLDL),[8,23–29] which is known to contain high levels of 7KCh.[12,13] The inflammatory pathways for 7KCh have been described in different cell types, and various inflammatory pathways have been implicated.[1–7] However, most of the cell types investigated respond to 7KCh by forming reactive oxygen species (ROS) with subsequent NFκB activation. The exception seems to be the human umbilical vein endothelial cell line ECV304 cells[30] and RPE-derived cells.[21,31] The ECV304 cell line is apparently not an endothelial cell line; rather, it originates from the T24 human bladder carcinoma cell line.[32]

Chronic inflammation is suspected of playing a role in drusen formation and the pathogenesis of age-related macular degeneration (AMD).[33] Inflammation also causes neovascularization, which is a major complication in a variety of ocular diseases.[33] VEGF is a key molecule in ocular neovascularization and is known to induce choroidal neovascularization (CNV) in AMD.[34] Presently, the most effective treatment for AMD with CNV is anti–VEGF therapy.[34] Thus, any molecule or process in the retina that regulates or induces VEGF is extremely important to the understanding of the disease process in AMD.

In this study we used the human RPE-derived ARPE-19 cell line to study the inflammatory mechanism of 7KCh. Our results suggest that 7KCh does not induce ROS in ARPE-19 cells or in other cell lines of various origin. Instead, 7KCh activates three kinase signaling pathways that lead to NFκB activation and subsequent cytokine induction.

Materials and Methods

Materials

7-Ketocholesterol was purchased from Steraloids, Inc. (Newport, RI). Hydroxypropyl-β-cyclodextrin (HPBCD), N-acetyl-L-cysteine (NAC), tert-butyl hydroperoxide (TBHP), and monoclonal anti–actin antibody were purchased from Sigma-Aldrich (St. Louis, MO). Cobalt chloride ($CoCl_2$) was purchased from J. T. Baker (Phillipsburg, NJ). Rabbit polyclonal antibodies specific for phospho-ERK, phospho-p38 MAPK, phospho-AKT, ERK, p38 MAPK, AKT, and phospho-PKCζ were obtained from Cell Signaling Technology Inc. (Boston, MA). Mouse mono-

From the Mechanisms of Retinal Diseases Section, Laboratory of Retinal Cell and Molecular Biology, National Eye Institute, National Institutes of Health, Bethesda, Maryland.

Supported by the National Eye Institute Intramural Research Program.

Submitted for publication November 2, 2009; revised March 30, 2010; accepted April 27, 2010.

Disclosure: **I.M. Larrayoz**, None; **J.-D. Huang**, None; **J.W. Lee**, None; **I. Pascual**, None; **I.R. Rodríguez**, None

Corresponding author: Ignacio R. Rodriguez, National Eye Institute, NIH, Section on Mechanisms of Retinal Diseases, LRCMB, 6 Center Drive, MSC0608, Bethesda, MD 20892; rodriguezi@nei.nih.gov.

Investigative Ophthalmology & Visual Science, October 2010, Vol. 51, No. 10

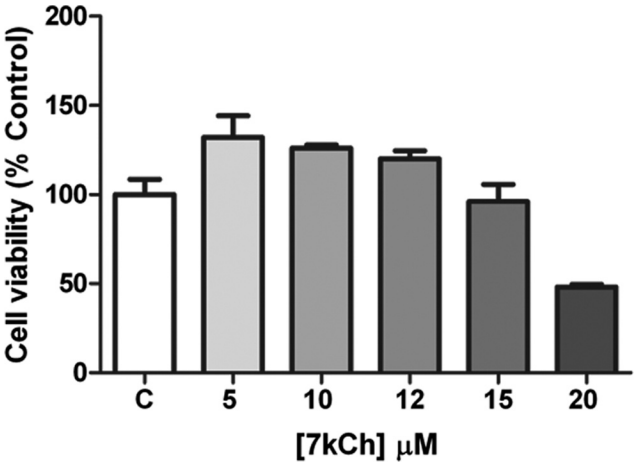

FIGURE 1. Cell viability in response to 7KCh treatment. ARPE-19 cells were incubated for 24 hours with the indicated concentrations of 7KCh. Cellular viability was determined by measuring dehydrogenase activity. Twenty-four well plates were used and four individual measurements were made for each concentration. Error bars are the SE from the four measurements. The figure shows a representative experiment repeated three times with similar results.

clonal anti–human HuR antibody was purchased from Santa Cruz Technology Inc. (Santa Cruz, CA). Rabbit polyclonal antibodies specific for β-tubulin and histone deacetylase 1 (HDAC1) were purchased from Abcam, Inc. (Cambridge, MA). U0126, SB203580, LY294002, myr-PKCζ, and BAY 11–7082 were purchased from EMD Chemicals Inc. (Gibbstown, NJ).

Cell Cultures and Treatments

ARPE-19 cells were purchased from the American Type Culture Collection (ATCC, Manassas, VA) and cultured as previously described.[8] The SV40-immortalized rat RPE-J cells[35] were a kind gift from George Hoppe (Cleveland Clinic, Cleveland, OH). These cells were cultured in Dulbecco's modified Eagle's medium (DMEM; Mediatech Inc., Manassas, VA) containing 4% FBS, 2 mM glutamine, 100 IU/mL penicillin, and 100 μg/mL streptomycin (Invitrogen Corp., Carlsbad, CA). Human microvascular endothelial cells (HMVECs)[36] were a kind gift from Rong Shao (Pioneer Valley Life Sciences Institute, Springville, MA). They were cultured and maintained in EBM-2 medium (Lonza, Basel, Switzerland) with supplements (10% FBS, 0.04% hydrocortisone, 0.1% rhEGF, 0.1% GA-1000, 100 IU/mL penicillin, and 100 μg/mL streptomycin). Human aorta smooth muscle cells (HAoSMC) were purchased from the ATCC. These cells were grown in DMEM containing 15% FBS, 2 mM glutamine, 100 IU/mL penicillin, and 100 μg/mL streptomycin. All cells were cultured at 37°C in 5% CO_2 with the exception of the RPE-J cells, which were grown at 32°C. Cells were treated with 7KCh complexed with HPBCD in serum-free media, as previously described.[8]

HuR Immunolocalization

For immunoblotting, ARPE-19 cells were treated with 15 μM of 7KCh for 0, 3, 6, and 12 hours. Cytoplasmic and nuclear fractions were prepared (Nuclear Extract Kit; Active Motif, Carlsbad, CA). Protein samples (40 μg for cytoplasmic extracts, 10 μg for nuclear extracts) were subjected to SDS-PAGE. Blots were probed overnight with anti–HuR antibody (1:1000) at 4°C. Anti–HDCA1 (1:10,000) and anti–β-tubulin (1:5000) antibodies were also used as a nuclear marker and a cytoplasmic marker, respectively. The blots were developed using anti–rabbit (KPL, Gaithersburg, MD) or anti–mouse

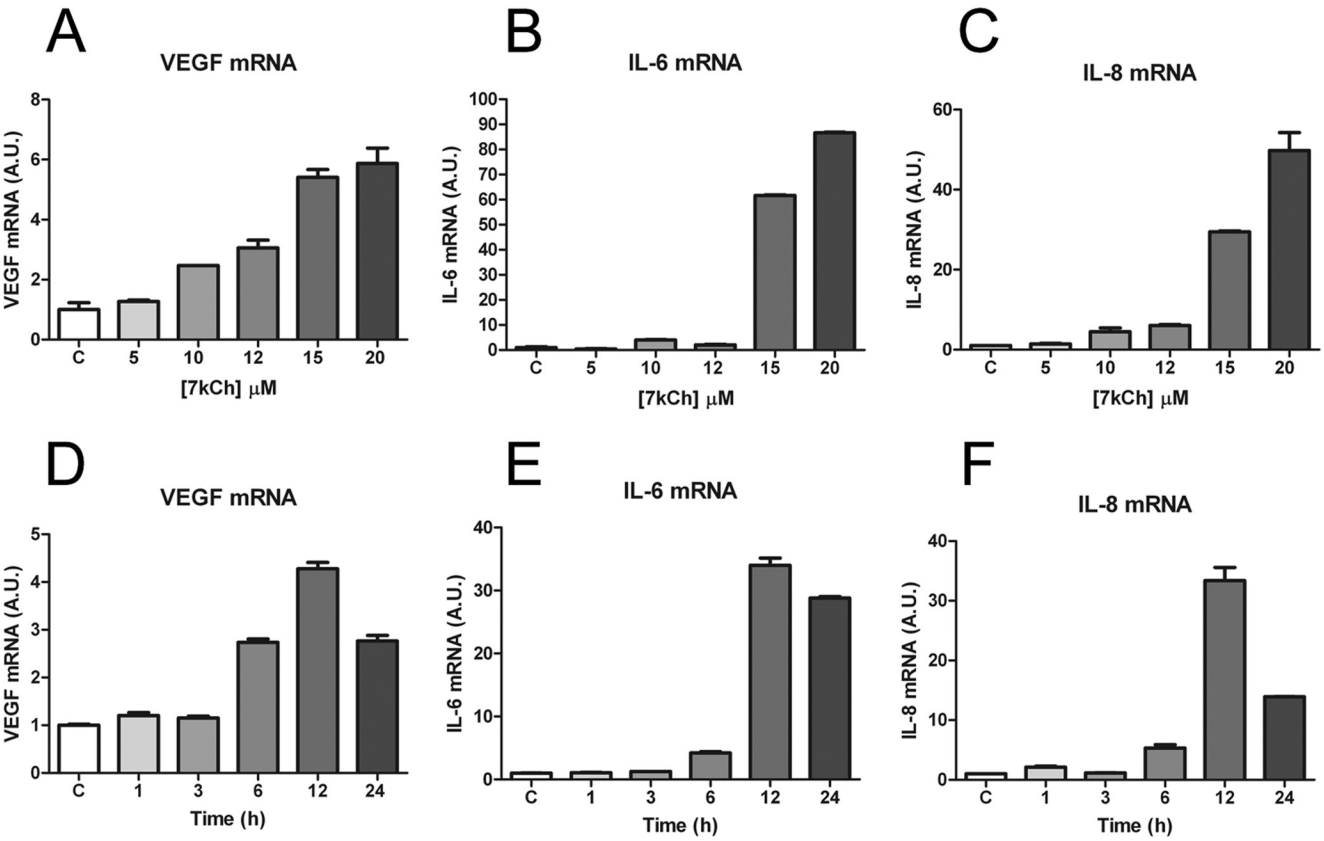

FIGURE 2. Dose and time response of cytokine mRNA induction by 7kCh. Dose-response for cytokine induction of VEGF (**A**), IL-6 (**B**), and IL-8 (**C**) mRNA in ARPE-19 cells exposed to 7KCh for 24 hours. Time course response for the induction of VEGF (**D**), IL-6 (**E**), and IL-8 (**F**) mRNA in ARPE-19 cells exposed to 15 μM 7KCh. Real-time qRT-PCR was performed. Error bars are the SE from four individual measurements. The figure shows representative experiments repeated three times with similar results.

(Jackson ImmunoResearch Laboratories, Inc., West Grove, PA) IgG peroxidase–conjugated secondary antibodies at a dilution of 1:10,000 for 1 hour, followed by incubation with the chemiluminescent substrate (SuperSignal West Pico; Thermo Fisher Scientific, Rockford, IL).

For localization by immunofluorescence, cells were seeded on two-well chamber slides (Laboratory-Tek; Nalgene Nunc International, Naperville, IL) and treated with 15 μM of 7KCh for 12 hours. Cells were washed with PBS and then fixed in PBS containing 4% paraformaldehyde for 15 minutes. Cells were washed again with PBS and blocked with 5% normal goat serum in ICC buffer (1% Triton X-100, 0.5% BSA, and 0.05% sodium azide in 1× PBS) for 30 minutes. Then the cells were incubated with anti–HuR antibody (1:100) in 2.5% normal goat serum-ICC buffer at room temperature for 2 hours. After washing with PBS, the cells were incubated with Alexa Fluor 488–labeled goat anti–mouse IgG (1:500; Invitrogen-Molecular Probes, Eugene, OR) and 1 μg/mL of 4′,6-diamidino-2- phenylindole (DAPI; Invitrogen-Molecular Probes) for 1 hour in the dark. After washing with PBS, the slides were mounted and imaged with a scanning confocal microscope (SP2; Leica Microsystems, Exton, PA).

cDNA Synthesis and Real-Time Quantitative RT-PCR

RNA extraction and cDNA synthesis were performed using reagents and kits (Invitrogen). All qRT-PCR experiments were performed three times in triplicate in a real-time PCR system (ABI 7500; Applied Biosystems, Foster City, CA) according to the manufacturer's specifications. Gene expression was quantified by using a PCR mix (SYBR Green PCR master mix; Applied Biosystems) and specific primers for IL-6 (forward, 5′-CCAGTACCCCCAGGAGAAGAT-3′; reverse, 5′-GAGGATGTACCGAATTTGTTTGTC-3′) and IκBα (forward, 5′-CGGACTGCCCTTCACCTC-3′; reverse, 5′-ACATCAGCCCCACACTTCAA-3′) or by using gene expression assays (hVEGFa, HS00173626_m1; hIL-8 HS00174103_m1; hNOX-4, HS00276431_m1; hGAPDH, 4352934e; rVEGFa, Rn00582935_m1, rIL-6, Rn99999011_m1; rNOX-4, Rn00585380_m1; rGAPDH, 4352338e; TaqMan; ABI Applied Biosystems). For each cDNA, GAPDH was used as an endogenous standard to estimate the mRNA levels. Results were normalized and expressed relative to standard controls and are shown as the average value, and the error bars are the SD from the mean.

Detection of Intracellular ROS

The level of intracellular ROS was determined by the change in fluorescence resulting from the oxidation of the fluorescent probe 2′, 7′-dichlorodihydrofluorescein diacetate (H2DCFDA; Invitrogen). ARPE-19 cells were exposed to 15 μM 7KCh for 0.5 to 24 hours. RPE-J cells, HMVECs, and HAoSMCs were exposed to various concentrations of 7KCh or $CoCl_2$ for 24 hours. After 7KCh treatment, cells were then incubated with 5 μM H2DCFDA at 37°C for 20 minutes. The fluorescence corresponding to intracellular ROS was determined using a multilabeled reader (Envision, model 2104; Perkin-Elmer, Waltman, MA) with 485-nm excitation and 535-nm emission filters.

Cell Viability Assays

Cell viability assays were performed in 24-well plates, with each measurement performed in quadruplicate. Cell viability was measured using a cell counting kit (Cell Counting Kit-8; Dojindo Molecular Technologies, Inc., Gaithersburg, MD), which measures cellular dehydrogenase (mostly mitochondrial) activity.

Immunoblots

Cells in 100-mm dishes were treated with 7KCh, alone or with inhibitors for 1, 3, 12, and 24 hours, and were extracted in MPER

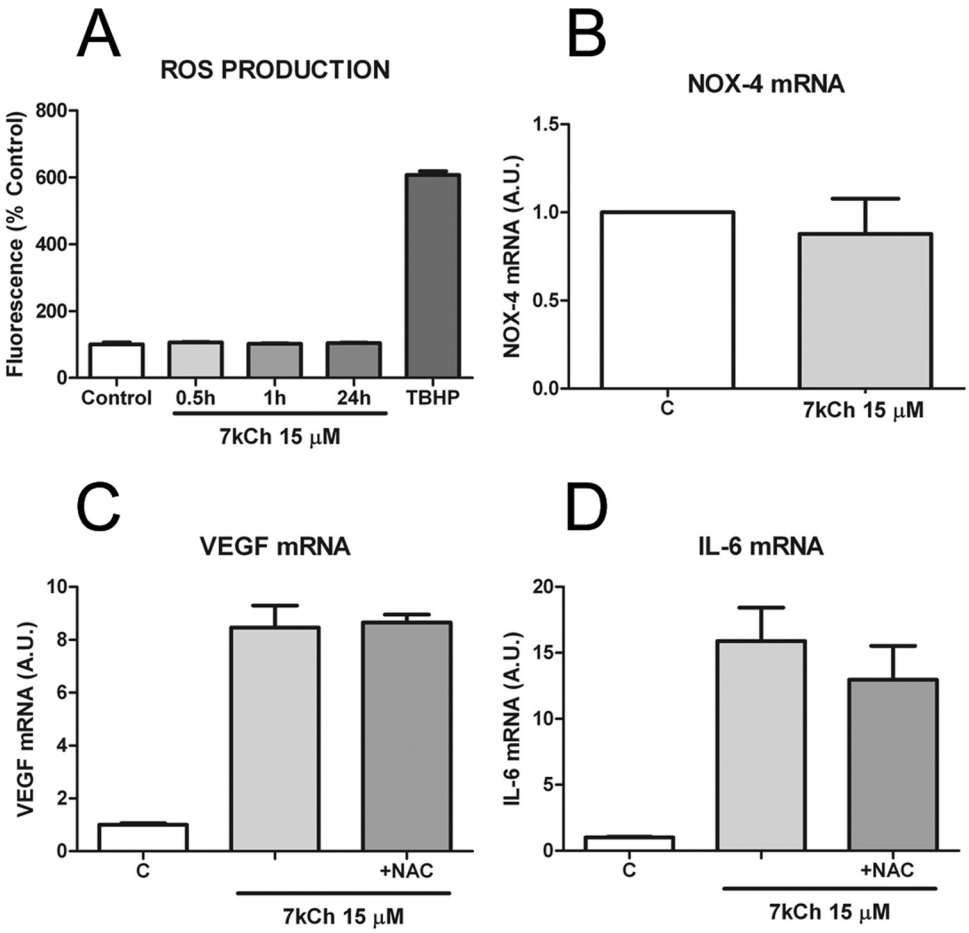

Figure 3. ROS production, NOX-4 induction, and cytokine response to 7KCh. ARPE-19 cells were treated with 15 μM 7KCh for 24 hours, and ROS production (**A**), NOX-4 mRNA induction (**B**), VEGF induction with and without NAC (**C**), and IL-6 induction with and without NAC (**D**) were measured. ROS was measured by fluorescence. NOX-4, VEGF, and IL-6 mRNA were measured by qRT-PCR in control and 7KCh-treated ARPE-19 cells (n = 5).

buffer solution (Thermo Fisher Scientific) in the presence of protease inhibitor cocktail (Complete; Roche Diagnostics Corporation, Indianapolis, IN). Protein samples from cell extracts (40 μg protein) were separated in a 10% Bis-Tris gel, transferred to a nitrocellulose membrane (Invitrogen), and probed with primary antibodies at 1:1000, 4°C overnight. The primary antibodies were anti–phospho-ERK, phospho-p38MAPK, phospho-AKT, ERK, p38 MAPK, AKT, and phospho-PKCζ. The blots were developed using HRP-conjugated secondary antibody at 1:2000 (Cell Signaling Technology, Inc.) and the chemiluminescent substrate (Supersignal West Pico; Thermo Fisher Scientific).

ELISA for VEGF, IL-6, and IL-8

Cytokine levels in conditioned media from ARPE-19 cells were measured 48 hours after treatment with 15 μM 7KCh. VEGF and IL-8 were quantified using the ELISA kits (human VEGF and human CXCL8/IL-8; Quantikine; R&D Systems, Inc., Minneapolis, MN). IL-6 was measured using a human IL-6 single analyte kit (ELISArray; SABioscience, Frederick, MD).

Results

Determining Optimal Inflammatory Concentration of 7KCh in 24 Hours

To determine the highest concentration of 7KCh that may be tolerated by ARPE-19 cells without cytotoxicity (cell death), different concentrations of 7KCh (0–20 μM) were tested for 24 hours in 24-well plates. Cellular dehydrogenase activity was used to determine cell viability, as described. Results indicate that concentrations of 7KCh up to 15 μM are not cytotoxic to ARPE-19 cells within 24 hours (Fig. 1). However, 20 μM 7KCh caused a 50% to 60% loss in cell viability (Fig. 1).

Dose and Time Dependence Induction of VEGF, IL-6, and IL-8 by 7KCh

The induction of VEGF, IL-6, and IL-8 mRNA by 7KCh was determined by real-time qRT-PCR as a function of the dose (Figs. 2A–C) and time (Figs. 2D–F) in ARPE-19 cells. Cells were

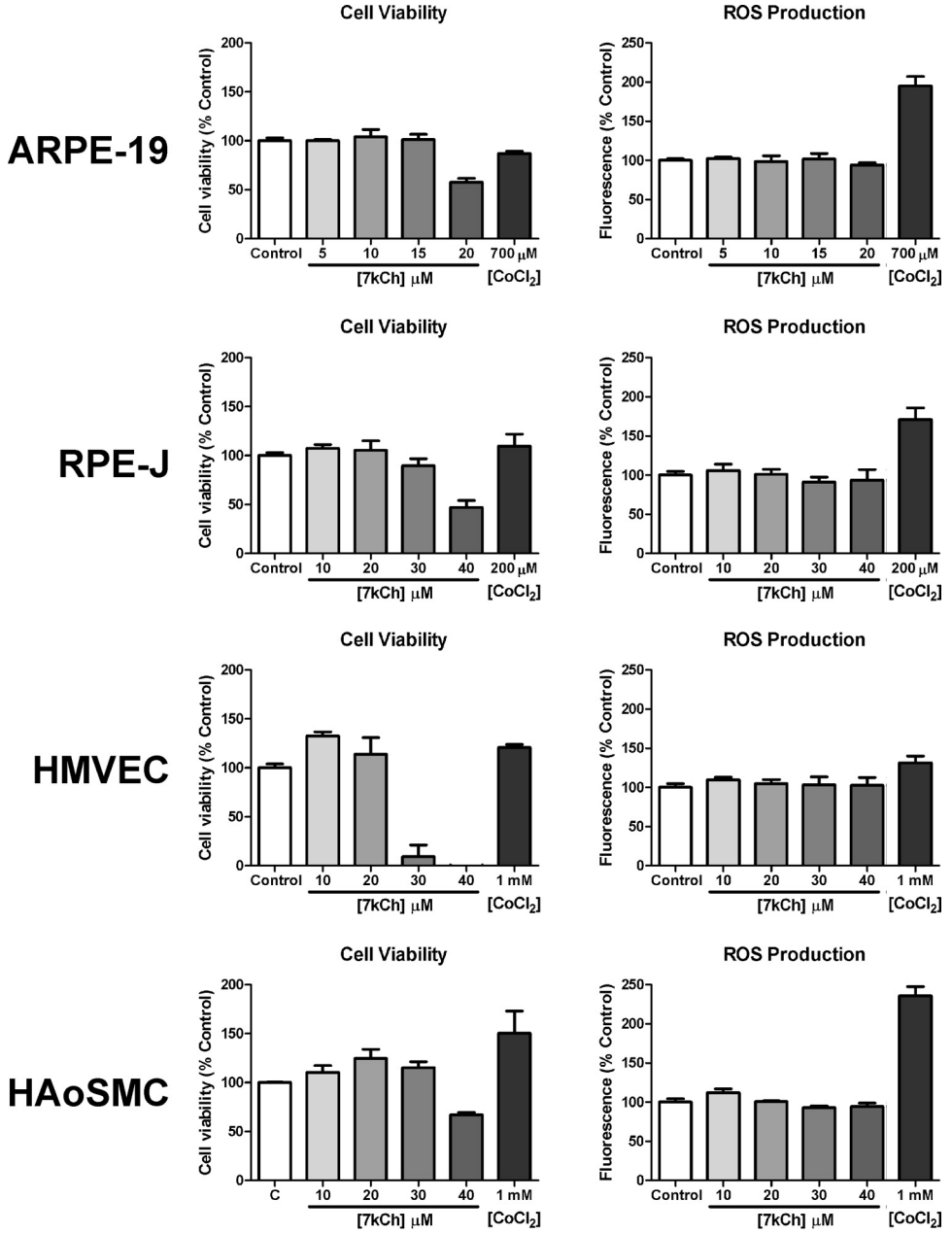

Figure 4. ROS production versus cell viability in different cell types. ARPE-19, RPE-J, HMVECs, and HAoSMCs were incubated with the indicated concentrations of 7KCh and $CoCl_2$ for 24 hours. The concentrations of $CoCl_2$ used were predetermined in previous experiments to optimize ROS production with minimal cytotoxicity. Error bars indicate SD from the mean of four independent measurements.

plated in 24-well plates, and measurements were performed in quadruplicate per experiment. Low doses of 7KCh (5–12 μM) were able to significantly induce the mRNA expression of VEGF and IL-8 mRNA whereas IL-6 required 15 μM. At 15 and 20 μM, all three cytokines were markedly induced (Fig. 2). In addition, all three cytokines responded to the 15 μM 7KCh by 6 hours with maximum induction at 12 hours. The 15-μM 7KCh dose was selected for subsequent studies because it provided the best balance between inflammatory response and cell toxicity.

ROS Formation and NOX-4 Induction in 7KCh-Treated ARPE-19 Cells

Studies performed in human aortic smooth muscle cells,[37] macrophages,[38] and human aortic endothelial cells[39] have shown that 7KCh induces VEGF and other cytokines through the generation of ROS. To determine whether the ARPE-19 cells responded similarly to 7KCh, the cells were incubated with 15 μM 7KCh for 0.5, 1, and 24 hours, and ROS production was measured as described (Fig. 3A). TBHP, a known ROS generator, was used as a positive control (Fig. 3A). Exposure to 7KCh did not cause any measurable ROS production or induce NOX-4 mRNA (Fig. 3B). Moreover, coincubation with N-acetylcysteine, a known ROS scavenger, did not block the induction of VEGF and IL-6 mRNA (Figs. 3C, 3D).

Because ROS formation has been reported in these other systems,[37–39] we examined one additional RPE-derived cell line (RPE-J) and two other cell lines, HMVECs and HAoSMCs, which had been previously shown to generate ROS in response to 7KCh.[37,38] Cell viability and ROS production were measured on all four cell lines under identical conditions (Fig. 4). Cobalt chloride was used as a positive control to generate ROS because it is significantly less toxic than TBHP. The optimal dose of $CoCl_2$ was determined for each cell line (data not shown) to maximize ROS production while maintaining good cell viability. None of the cell lines demonstrated any significant increase in ROS production (Fig. 4) or NOX-4 induction (data not shown) in response to 7KCh exposure.

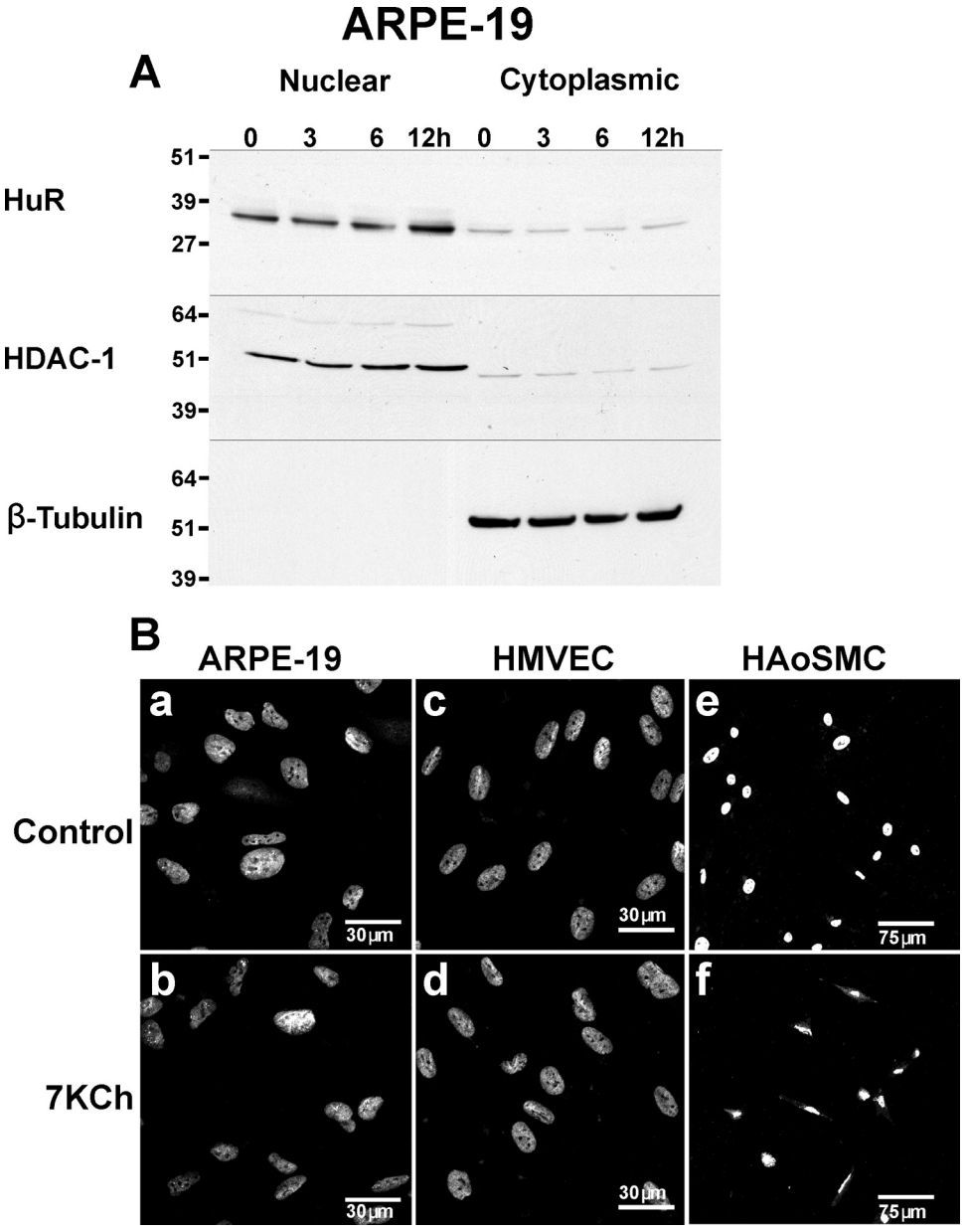

FIGURE 5. HuR induction and translocation in response to 7KCh. (**A**) HuR immunoblot of cytosolic and nuclear extracts of ARPE-19 cells after treatment with 15 μM 7KCh for 0, 3, 6, and 12 hours. (**B**) Localization of HuR by immunofluorescence before (**Ba**, **Bc**, **Be**) and after (**Bb**, **Bd**, **Bf**) treatment with 15 μM 7KCh for 12 hours. ARPE-19 (**Ba**, **Bb**), HMVECs (**Bc**, **Bd**), and HAoSMCs (**Be**, **Bf**).

Expression and Translocation of HuR Protein in Response to 7KCh

HuR is an RNA-binding protein that stabilizes the adenylate-uridylate rich elements present in different proinflammatory mRNAs such as IL-6.[40] HuR translocates from the nucleus to the cytosol by an NFκB signaling response.[41] In HAoSMCs, 7KCh has been previously shown to cause the translocation of HuR.[18]

To determine whether HuR was involved in 7KCh-mediated cytokine induction, ARPE-19 cells were incubated with 15 μM 7KCh for 0, 3, 6, and 12 hours. Cytosolic and nuclear fractions were prepared and analyzed by immunoblot to determine HuR translocation. The cytosolic marker β-tubulin and the nuclear marker HDAC1 were used as controls (Fig. 5A). No translocation of HuR was observed in ARPE-19 cells in response to 7KCh (Fig. 5A). Immunofluorescence localization also failed to detect HuR translocation in ARPE-19 cells or HMVECs (Figs. 5Ba–Bd). However, HAoSMC, our positive control, did show HuR translocation in response to 7KCh (Figs. 5Be, 5Bf), as previously reported.[18]

Involvement of the MAPK/ERK Pathway

The MAPK/ERK pathway is a complex signaling cascade activated by a variety of G-protein–coupled cell surface receptors in response to growth factors and other stimuli.[42,43] This pathway has been reported to regulate 7KCh-induced apoptosis.[44] To determine whether the MAPK/ERK pathway is involved in 7KCh-induced cytokine induction, ARPE-19 cells were incubated for 1, 3, 12, and 24 hours with 15 μM 7KCh. Changes in the expression and phosphorylation of ERK (pERK) were measured by immunoblot (Fig. 6A) using specific antibodies to the different forms. The expression of nonphosphorylated ERK (Fig. 6A, middle panel) was not affected, but increased phosphorylation was detected after 1 hour of treatment (Fig. 6A, top panel) and peaked after 3 hours. The levels of pERK remained elevated for 24 hours after treatment with 7KCh (Fig. 6A, top panel). β-Actin was used as a control for loading (Fig. 6A, lower panel). Pharmacologic inhibition of the ERK kinases Erk1 and Erk2, with the highly selective inhibitor U0126,[45,46] reduced VEGF, IL-6, and IL-8 mRNA levels by approximately 70%, 60%, and 50%, respectively (Figs. 6B–D).

To further elucidate the involvement of the MAPK/ERK pathway[43] in the 7KCh-induced cytokine response, ARPE-19 cells were incubated for 1, 3, 12, and 24 hours with 15 μM 7KCh, and p38MAPK phosphorylation was measured by immunoblot (Fig. 7A). As with the ERKs, nonphosphorylated p38MAPK expression was not altered, but phosphorylated p38MAPK expression increased within 1 hour and peaked after 3 hours. Phosphorylated p38MAPK levels remained elevated even 24 hours after treatment (Fig. 7A). Inhibition of the p38MAPK with the highly selective inhibitor SB203580[46] significantly reduced the cytokine induction. Inhibition of p38MAPK reduced the 7KCh-mediated induction of VEGF, IL-6, and IL-8 mRNA by approximately 50%, 70%, and 50%, respectively (Figs. 7B–D).

Involvement of the Akt/PKB Signaling Pathway

The serine/threonine kinase (Akt, also known as PKB) is known to play a critical role in diverse cellular processes.[47]

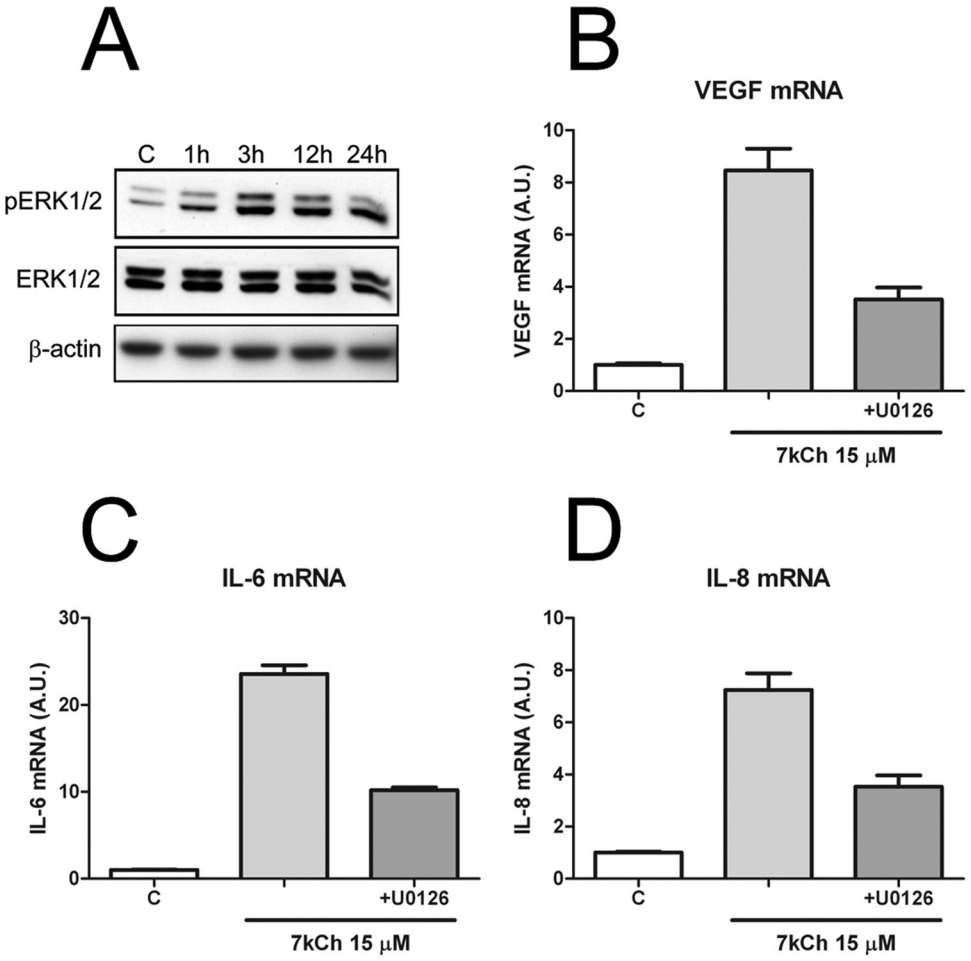

FIGURE 6. MEK-ERK phosphorylation and cytokine induction in response to 7KCh. (**A**) Immunoblot measuring the levels of phosphorylated and total forms for p42/44 (ERK) in ARPE-19 cells at 0, 1, 3, 12, and 24 hours after the addition of 15 μM 7KCh. (**B**) VEGF. (**C**) IL-6. (**D**) IL-8. Cytokine mRNA expression was measured by qRT-PCR 24 hours after the addition of 15 μM 7KCh with and without the MEK inhibitor U0126. The inhibitor was dissolved in DMSO and used at a final concentration of 10 μM. Error bars are the SE from four individual measurements. The figure shows a representative experiment repeated three times with similar results.

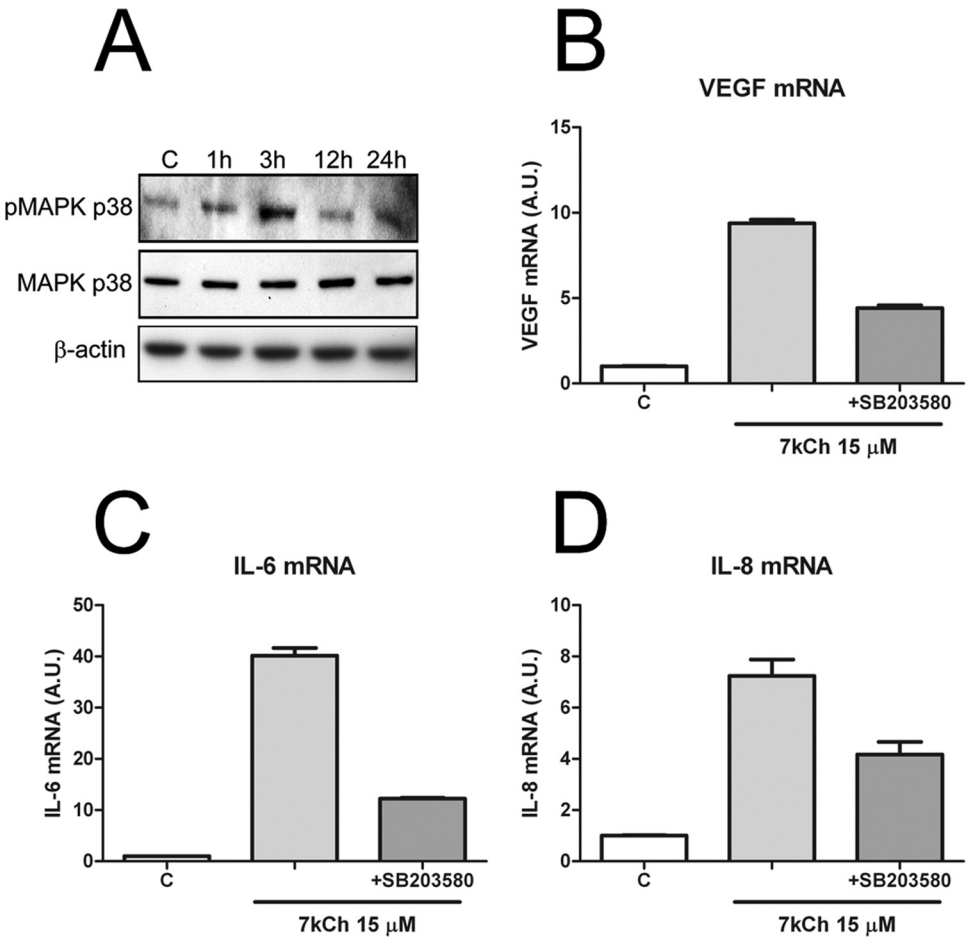

FIGURE 7. MAPK P38 phosphorylation and cytokine induction in response to 7KCh. (**A**) Immunoblot measuring the levels of phosphorylated and total forms for P38 at 0, 1, 3, 12, and 24 hours after the addition of 15 μM 7KCh. (**B**) VEGF. (**C**) IL-6. (**D**) IL-8. Cytokine mRNAs were measured by qRT-PCR 24 hours after treatment with 15 μM 7kCh with and without the MAPK inhibitor SB203580. The inhibitor was dissolved in DMSO and used at a final concentration of 10 μM. Error bars are the SE from four individual measurements. The figure shows a representative experiment repeated three times with similar results.

Akt is activated by a variety of cell surface receptors that, when stimulated, induce the activation of the enzyme phosphoinositide 3-kinase (PI3K). PI3K produces phosphatidylinositol 3, 4, 5 triphosphates (PIP3), which in turn activates Akt.[47] To determine whether Akt signaling was involved in the 7KCh-induced cytokine induction, ARPE-19 cells were incubated with 7KCh under conditions identical to those described above for MAPK/ERK. The expression and phosphorylation of Akt were measured by immunoblot (Fig. 8A) using specific antibodies that can distinguish phosphorylated and nonphosphorylated forms of Akt. Similar to MAPK/ERK levels, nonphosphorylated Akt levels did not seem to vary, but phosphorylated Akt (pAkt) increased within 1 hour after treatment and peaked at 12 hours (Fig. 8A). The Akt and PI3K inhibitor LY294002[48] attenuated the induction of VEGF, IL-6, and IL-8 mRNA by approximately 75%, 80%, and 50%, respectively (Figs. 8B–D).

Involvement of Protein Kinase C

Previous studies have implicated protein kinase C (PKC) isoforms in the induction of VEGF and other cytokines.[47,49] We were unable to detect either PKCδ or PKCθ phosphorylation in 7KCh-treated ARPE-19 cells by immunoblot (data not shown). However, a time-dependent increase in the phosphorylation of PKCζ was detected by immunoblot in 7KCh-treated ARPE-19 cells (Fig. 9A). Moreover, incubation with myr-PKCζ, a myristoylated form of the PKCζ isozyme and a pseudo-substrate inhibitor, blocked 7KCh-mediated VEGF, IL-6, and IL-8 mRNA induction by 60%, 75%, and 70%, respectively (Figs. 9B–D).

Involvement of NFκB

The nuclear factor NFκB is a family of five related proteins that form homodimers and heterodimers.[50] In resting cells the NFκB dimers form complexes with small inhibitory proteins called IκBs. An essential step in the activation of the NFκB complex is the phosphorylation and activation of the IκB kinase complex (IKK), which phosphorylates the inhibitor IκBs. IKK is a trimeric complex composed of IKKα and β catalytic subunits and the IKKγ regulatory subunit.[50] The phosphorylation of the IκBs causes their ubiquitination and degradation, thus freeing the NFκB complex. Ubiquitination plays an essential role in the regulation of NFκB.[51] The freed NFκB dimers are then phosphorylated and translocated to the nucleus to promote the transcription of many immunity-related genes, including the IκB genes.[50,51] This creates a negative feedback loop leading to the induction and resynthesis of the IκBs. Hence, the induction of IκBα mRNA expression is considered a reliable marker for measuring the activation of the NFκB pathway.[50,52]

Treatment of ARPE-19 cells with increasing doses of 7KCh for 24 hours demonstrated that the expression of IκBα mRNA increased in a dose-dependent manner (Fig. 10A). Treatment of ARPE-19 cells with 15 μM 7KCh demonstrated that IκBα mRNA expression peaks 6 hours after treatment (Fig. 10B) and remains elevated for 24 hours (last measurement). Moreover, incubation with 2 to 10 μM BAY 11–7082, an irreversible inhibitor of IKK,[53] blocked the 7KCh-mediated induction of IκBα mRNA (Fig. 10C). The BAY 11–7082 also practically ablated 7KCh-mediated cytokine induction (Figs. 10D–F).

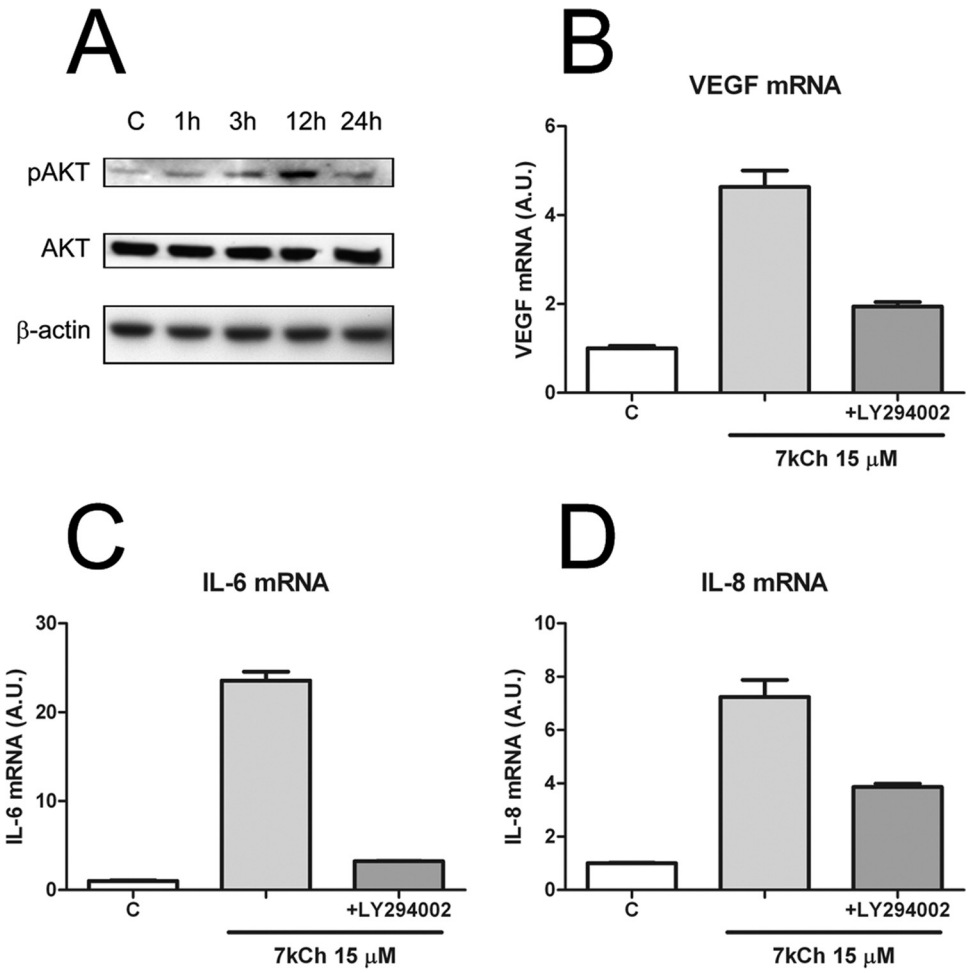

FIGURE 8. PI3K-AKT phosphorylation and cytokine induction in response to 7KCh. (**A**) Immunoblot measuring the levels of phosphorylated and total forms for AKT at 0, 1, 3, 12, and 24 hours after the addition of 15 μM 7KCh. (**B**) VEGF. (**C**) IL-6. (**D**) IL-8. Cytokine mRNAs were measured by qRT-PCR 24 hours after treatment with 15 μM 7kCh with and without the PI3K inhibitor LY294002. The inhibitor was dissolved in DMSO and used at a final concentration of 10 μM. Error bars are the SE from four individual measurements. The figure shows a representative experiment repeated three times with similar results.

NFκB Activate Independently of MAPK/ERK

To determine the pathway location of NFκB activation, IκBα mRNA was measured in the 7KCh-treated ARPE-19 cells in the presence of all the different inhibitors tested (Fig. 11A). The inhibitors of p38MAPK (SB203580) and ERK (U0216) had essentially no effect on IκBα mRNA induction by 7KCh. However, the inhibition of PI3K (LY294002) and PKCζ (myr-PKCζ) measurably depressed IκBα mRNA expression (Fig. 11A). These results suggest that in ARPE-19 cells, 7KCh-mediated activation of the MAPK/ERK pathways influence cytokine induction mainly downstream of NFκB.

Cytokine Protein Expression

Given that mRNA expression does not necessarily correlate with protein expression, ELISA was used to determine the release of VEGF, IL-6, and IL-8 into the medium after 7KCh treatment. ARPE-19 cells were treated with 7KCh (15 μM, 48 hours), and the levels of each cytokine were measured with and without the inhibitors U0126, SB203580, LY294002, BAY 11–7082, and myr-PKCζ (Figs. 11B–D). All five inhibitors attenuated the response to VEGF (Fig. 11B), IL-6 (Fig. 11C), and IL-8 (Fig. 11D). Results indicate that the mRNA levels correlate well with the protein release into the conditioned media and further support the involvement of NFκB in cytokine expression.

DISCUSSION

This study is a continuation of a previous study[8] to determine the mechanisms of 7KCh-mediated inflammation and cytotoxicity in RPE cells. Determining the signaling pathways involved in the 7KCh-mediated cytokine induction in vitro will be useful in guiding investigative strategies for more definitive studies in vivo. The cytotoxicity and inflammatory mechanisms for 7KCh have been extensively studied in a variety of cultured cell types.[1–7] Most of the previously published work on this subject has been on macrophage- , smooth muscle- and vascular endothelial-derived cell lines, which have been reported to respond by way of ROS-mediated pathways.[1,3] In this study we demonstrate that ARPE-19 cells respond similarly to 7KCh but independently of NOX-4 and ROS induction. This study also suggests that 7KCh activates multiple signaling pathways (AKT-PKCζ, ERK, and p38 MAPK) that lead to NFκB activation and cytokine expression.

We have found that in ARPE-19 cells, 7KCh doses between 15 and 20 μM worked best for cytokine induction without excessive cytotoxicity (Fig. 1). The 7KCh-mediated cytokine mRNA induction was clearly detectable with 10 μM for all three cytokines tested—VEGF, IL-6, and IL-8 (Figs. 2A–C, respectively). Cytokine induction was detected within 6 hours after 7KCh treatment, but peak response occurred at 12 hours for all cytokines (Figs. 2D–F).

The mechanism(s) by which 7KCh induces inflammation have been studied in human fibroblasts,[54] human aortic and embryonic vascular endothelial cells (HUVECs),[8,16,54,55] cultured neuroretinal cells,[56] human monocytic U937 cells,[57–60] THP-1 cells,[44] aortic smooth muscle cells,[18,37,54,60,61] human macrophages,[20,38,62] and human RPE cells.[8,27] In aortic smooth muscle cells, 7KCh has been reported to induce the expression and activity of NOX-4, which in turn increases the formation of

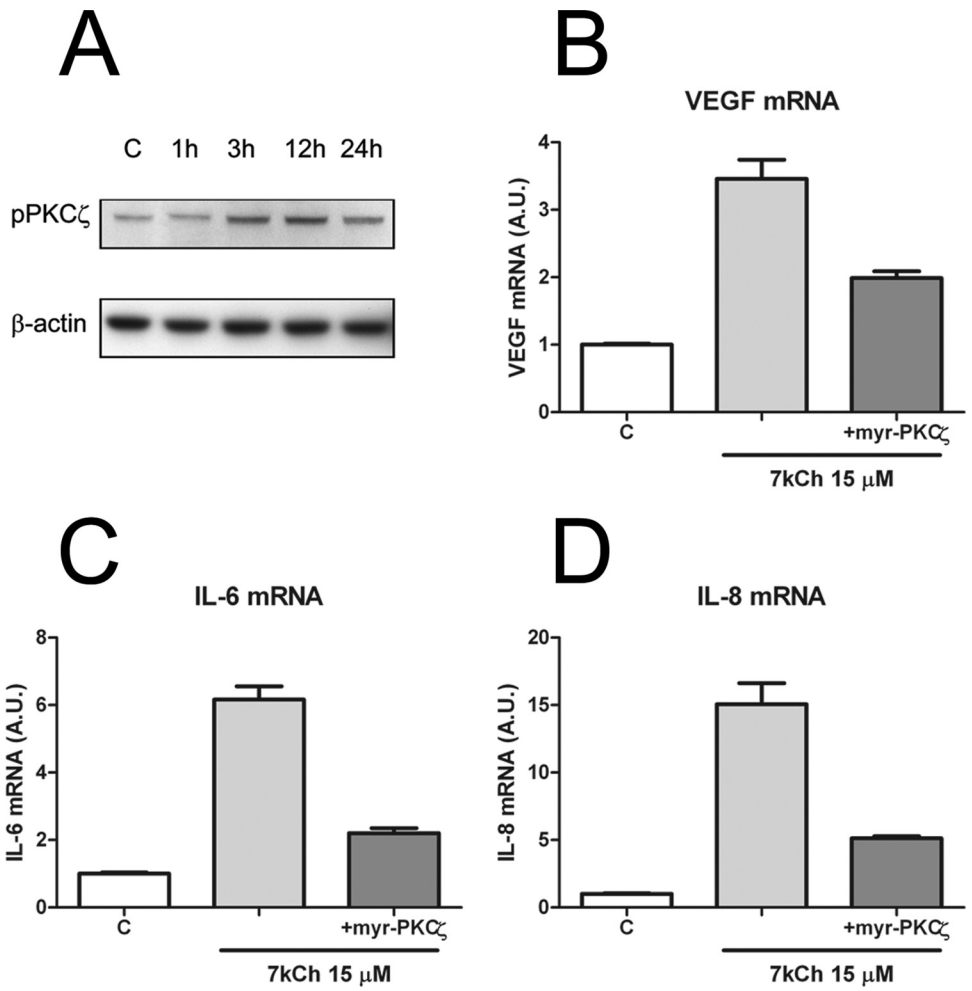

FIGURE 9. PKCζ phosphorylation and cytokine induction in response to 7KCh. (**A**) Immunoblot measuring the levels of phosphorylated PKCζ 0, 1, 3, 12, and 24 hours after the addition of 15 μM 7kCh. (**B**) VEGF. (**C**) IL-6. (**D**) IL-8. Cytokine mRNAs were measured by qRT-PCR 24 hours after treatment with 15 μM 7kCh with and without the pseudo-substrate inhibitor Myr-PKCζ. The inhibitor was dissolved in water and used at a final concentration of 20 μM. Error bars are the SE from four individual measurements. The figure shows a representative experiment repeated three times with similar results.

ROS.[37] In the mouse J774A.1 macrophage cell line, 7KCh was demonstrated to induce apoptosis by increasing ROS formation and caspase-3 activity.[62] ROS formation is known to activate a series of proapoptotic pathways (Bax, p53, p21, phosphorylated JNK, and others) and to downregulate antiapoptotic genes (BcL-2, BcL-xL, AKT).[38] In the human macrophage THP-1 cell line, 7KCh treatment increased the phosphorylation of p38 MAPK and ERK and decreased total AKT protein.[38] In cultured human aortic endothelial cells, ROS-dependent translocation of NFκB into the nucleus was observed 2 hours after 7KCh exposure.[39] In these cell types, the pharmacologic effects elicited by 7KCh seem to be preceded by the formation of ROS. The prevention of ROS formation by antioxidants such as β-carotene,[38,63] treatment with NOX-4 inhibitors (diphenyleneiodonium chloride, DPI), or siRNA targeting are sufficient to block all the downstream effects of 7KCh.[37] In the RPE-derived cells, ROS formation does not seem to be involved in the 7KCh-induced inflammatory response or cell death (Fig. 3). ARPE-19 cells treated with 15 μM 7KCh failed to form ROS (Fig. 3A) or to induce NOX-4 (Fig. 3B). Moreover, treatment with N-acetylcysteine (a known ROS scavenger) failed to attenuate the 7KCh-induced VEGF response (Fig. 3C). Other investigators have also previously demonstrated that 7KCh did not increase ROS formation in ARPE-19 cells, even at concentrations in excess of 100 μM.[31] To further verify this result, we measured ROS formation in RPE-J cells, HMVECs, and HAoSMCs using $CoCl_2$ as a positive control (Fig. 4). 7KCh failed to induce ROS formation or NOX-4 induction (data not shown) in any of the four cell types tested. Other investigators using primary porcine RPE cells observed an increase in ROS formation in response to 7KCh[21] but concluded that the cytokine induction was mediated by LXR, not by ROS.

Why 7KCh did not seem to induce ROS in any of the cell types tested in our study is unclear. One possible explanation may be the way we delivered 7KCh. We used a complex with HPBCD, whereas others have used ethanol. In 4.5% HPBCD, 7KCh remained soluble in the culture media. In ethanol, 7KCh precipitated forming a suspension that adhered to the plastic surfaces or that precipitated on top of the cells. In HPBCD, we were also able to obtain pharmacologic responses in the 5- to 15-μM range, whereas in ethanol other investigators used concentrations in excess of 50 μM. This ethanol combination may lead to increased damage to the plasma membrane and perhaps to mitochondrial depolarization, which in turn leads to ROS formation.

In human vascular smooth muscle cells, a novel mechanism for the 7KCh-mediated induction of IL-6 through the translocation of the protein HuR from the nucleus to the cytoplasm was recently reported.[18] HuR is an RNA-binding protein known to stabilize the mRNA of various genes, including cytokines, by binding to adenylate-uridylate rich elements in their 3′ untranslated regions.[40,41] HuR mRNA expression is also controlled by NFκB.[18,41] We found no change in HuR expression or translocation in the 7KCh-treated ARPE-19 cells (Figs. 5A, Ba, Bb). HMVECs also failed to translocate HuR in response to 7KCh (Figs. 5Bc, Bd). However, the HAoSMCs (Figs. 5Be, Bf) did demonstrate HuR translocation in response to 7KCh. This result served as a positive control and confirmed previously published work.[18] HuR has also been shown to promote the translation

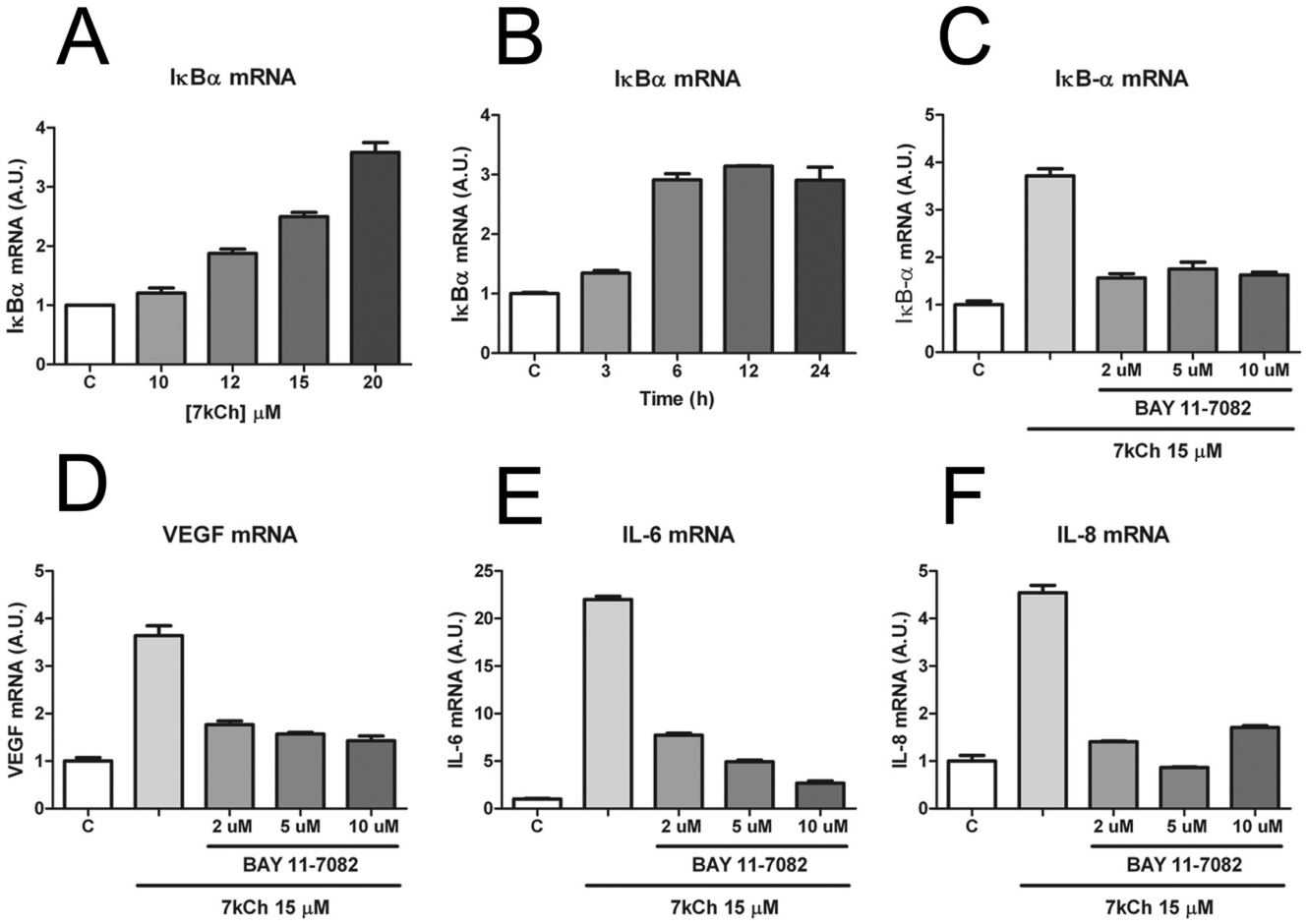

FIGURE 10. IκBα induction by 7KCh and inhibition by BAY 11–7082. (**A**) Dose-response curve for IκBα mRNA after 24 hours treatment with 7KCh in ARPE-19 cells. (**B**) Time course of IκBα mRNA induction by 15 μM 7kCh. (**C**) Inhibition of the 7KCh-mediated IκBα mRNA induction by BAY 11–7082. (**D**) VEGF. (**E**) IL-6. (**F**) IL-8. IκBα and the cytokines mRNA were measured by qRT-PCR. Error bars are the SE from four individual measurements. The figure shows a representative experiment repeated four times with similar results.

of HIF-1α,[64] which is the main protein controlling the transcriptional induction of VEGF.[65] However, we have previously demonstrated that HIF-1α is not involved in the 7KCh-mediated VEGF induction in ARPE-19 cells.[8] In addition, the NFκB inhibitor BAY 11–7082 ablated all the 7KCh-mediated cytokine responses (Fig. 11). This suggests that the HuR response to 7KCh may be dependent on cell type-specific PKC responses[18,41] that may not be present in HMVECs or ARPE-19 cells.

7KCh-mediated inflammatory responses in ARPE-19 cells do have some similarities to those observed in other cells types. 7KCh induces the phosphorylation of ERK (Fig. 6) and p38MAPK (Fig. 7) similarly to what was previously observed in the human macrophage-derived THP-1 cell line.[38] However, unlike the THP-1 cells,[38] 7KCh did activate the AKT pathway in the ARPE-19 cells (Fig. 8). Thus, in human macrophages, the downregulation of the AKT pathway is associated with cell death, whereas in ARPE-19 cells we observed a slight increase in cell proliferation with low doses of 7KCh (Fig. 1). Consistent with these observations, the pharmacologic inhibition of MEK-ERK (Figs. 6, 11), p38 MAPK (Figs. 7, 11), and PI3K-AKT (Figs. 8, 11) pathways significantly attenuated the 7KCh-mediated cytokine responses.

The role of different PKC isoforms (approximately 11) has been associated with the activation of proinflammatory signaling and the production of VEGF and other cytokines in different systems.[47,49,66,67] PKCα has been demonstrated to directly phosphorylate the HuR protein and to induce its translocation to the cytoplasm in cultured human mesangial cells.[41] Activation of PKCδ, which is promoted by oxysterols,[67] can induce the generation of ROS in cultured human neutrophils.[68] PKCζ , by contrast, works in conjunction with AKT to activate the NFκB complex without ROS formation.[69] The phosphoinositide-dependent kinase 1 (PDK1) phosphorylates both PKCζ and AKT. AKT then phosphorylates the IKK complex, and PKCζ phosphorylates NFκB.[69] Our data demonstrate that 7KCh induces the phosphorylation of PKCζ in a time-dependent manner, and this activation is responsible for a significant part of the cytokine induction observed (Fig. 9). This is in agreement with previously published results demonstrating that the oxLDL-mediated induction of VEGF secretion by macrophage-derived cell lines was dependent on PI3K and PKCζ but independent of other PKC isoforms or oxLDL uptake.[29] The response by these cells without oxLDL uptake suggests 7KCh (and other oxidized lipids) may exchange from the oxLDL particles to cellular membranes and induce inflammation just by direct contact.[29] Cellular stretch in retinal capillary pericytes also induced VEGF by PKCζ but independently of Akt, other PKC isoforms, Ras, and ERK1/2.[69] Moreover, the incubation of ARPE-19 cells with the calcium channel blocker APB or with EGTA, a calcium-chelating agent, did not affect the expression of VEGF, IL-6, and IL-8

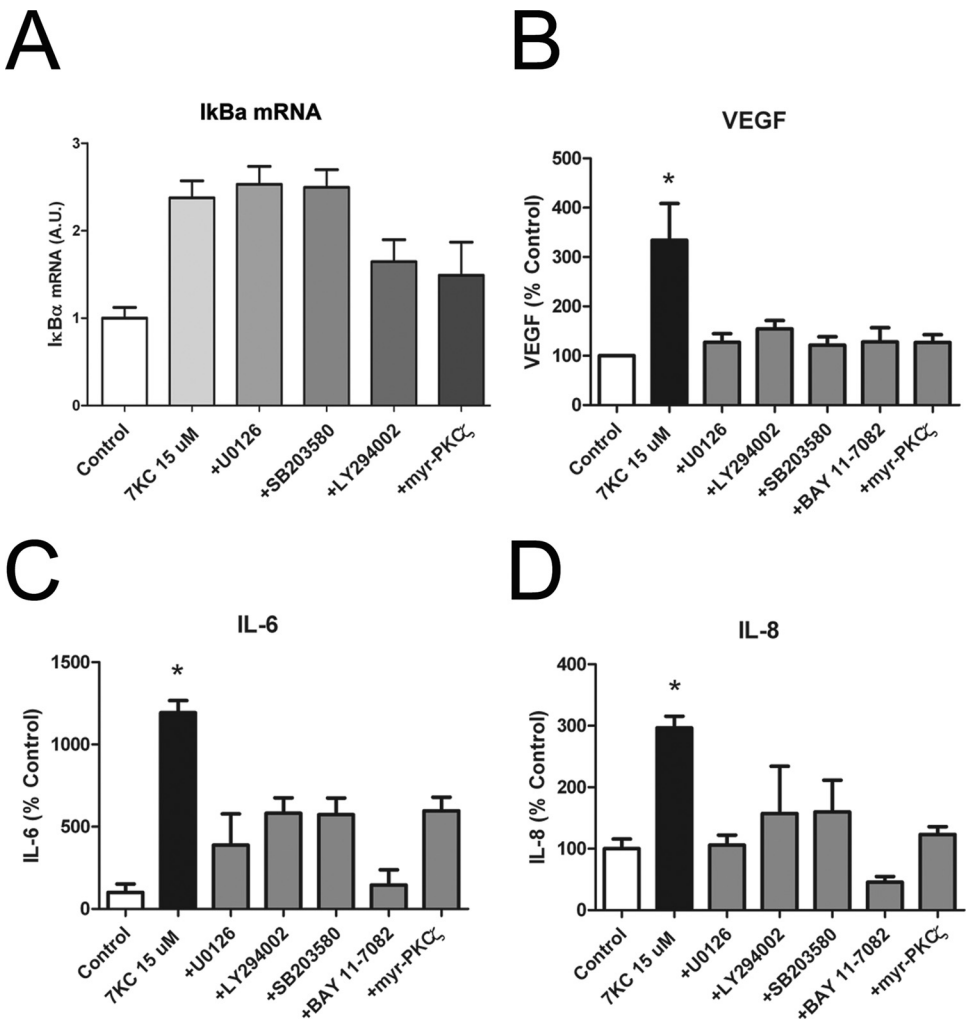

FIGURE 11. Effect of kinase inhibitors on IκBα mRNA and on cytokine protein expression. (**A**) IκBα mRNA was measured by qRT-PCR 24 hours after treatment with 15 μM 7KCh in the presence of the MEK inhibitor U0126 (10 μM), the p38MAPK inhibitor SB203580 (10 μM), the PI3K inhibitor LY294002 (10 μM), and the PKCζ inhibitor myr-PKCζ (20 μM). (**B**) VEGF. (**C**) IL-6. (**D**) IL-8. Cytokine release was measured by ELISA in the conditioned media of the ARPE-19 cells 48 hours after treatment with 15 μM 7KCh with and without the inhibitors. The figure shows a representative experiment repeated three times with similar results.

(data not shown). We also failed to detect the phosphorylation of δ or θ in ARPE-19 cells (data not shown). Thus, other PKC isoforms do not seem to be involved in the 7KCh-mediated cytokine induction in ARPE-19 cells, though they may be involved in HuR translocation in other cell types (e.g., HAoSMCs; Fig. 12).

NFκB is a family of five transcription factors that form homodimers and heterodimers known to control the expression of cytokines and other immune-response genes.[50,51] The NFκB dimers are kept inactive by the binding of the inhibitory proteins, the IκBs. NFκB activation requires phosphorylation of the IκBs by the IKK complex, followed by ubiquitination and proteasomal degradation of the IκB components.[51] This frees NFκB to form dimers that are further activated by phosphorylation and subsequently are translocated to the nucleus.[50] In the nucleus they work independently or in combination with other transcription factors to induce the expression of cytokine and other genes. NFκB activation is dependent on a balance between ubiquitination and degradation of the IκBs and the NFκB-dependent resynthesis of the IκBs.[50,51] We have demonstrated that 7KCh induces the expression of IκBα (Figs. 10, 11), which serves as a marker for NFκB activation.[50–52] The induction of IκBα by 7KCh is fast and dose-dependent (Fig. 10), paralleling the activation of the kinases (ERK, p38MAPK, AKT) (Figs. 6–8). However, specific inhibitors of p38MAPK (SB203580) and ERK (U0126) did not show the inhibition of IκBα mRNA induction (Fig. 10), whereas inhibition of PI3K (LY294002) and PKCζ (myr-PKCζ) demonstrated a marked inhibition of IκBα mRNA expression (Fig. 11). In addition, inhibition of the IKK-complex (BAY 11–7082) essentially ablated the mRNA expression of IκBα (Fig. 10) and of all three cytokines tested (Fig. 11). This indicates that NFκB activation is essential to the 7KCh-mediated cytokine induction while p38MAPK and ERK predominantly modulate NFκB activity through the expression or activation of other transcription factors. An illustration summarizing the 7KCh-mediated inflammatory pathways involved and the location of the inhibitors is shown (Fig. 12).

One important question that should be addressed is the physiological concentrations of 7KCh. In atheromatous plaques, 7KCh can reach concentrations greater than 100 μM,[13,70] with a significant portion of it as fatty acid esters.[12,13] Lipoprotein deposits are highly enriched in cholesterol esters, which are readily oxidized by a free radical–mediated mechanism catalyzed by copper, iron, or both.[12,14] Therefore, it would be safe to assume that cells in the vicinity of lipoprotein deposits could be exposed to micromolar amounts of 7KCh.

Another is how 7KCh activates these pathways. Are the high concentrations enough to trigger the cell surface receptors? Perhaps some of the G-protein–coupled receptors that respond to steroid hormones and activate MAPK/ERK may be fooled by high concentrations of a ketosteroid. However, it is unlikely the plethora of other receptors that trigger these inflammatory pathways could be activated by 7KCh. One possibility that has been alluded to in the published literature is the formation of 7KCh microcrystals in the plasma membrane.[71,72] However, to our knowledge, there are no published reports demonstrating that 7KCh microcrystals can trigger inflammatory receptors. Thus, the

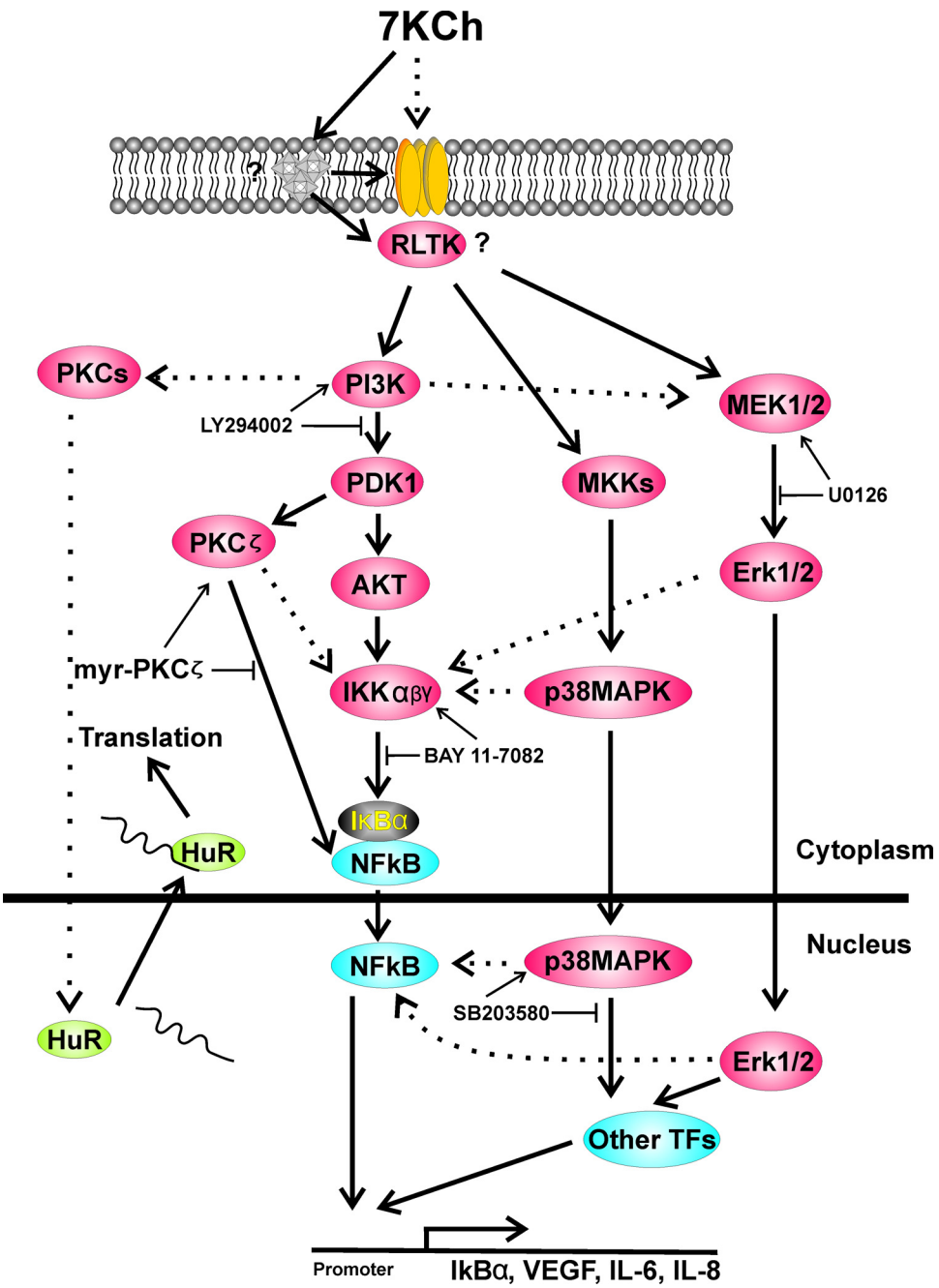

FIGURE 12. Proposed 7KCh-mediated cytokine activation pathways in ARPE-19 cells. 7KCh exchanges in the plasma membrane and causes the activation of the inflammatory pathways by some unknown mechanism (e.g., perhaps microcrystal formation). Interaction with the plasma membrane activates the cell surface receptors and/or the receptor-linked tyrosine kinases (RLTKs) by an unknown mechanism. *Dashed lines*: putative and/or inefficient phosphorylations. *Solid arrows*: suggested main flow of the pathways.

mechanism by which 7KCh activates these inflammatory pathways remains unknown and will be the focus of our future research.

The role that 7KCh may play in the pathogenesis of AMD is intriguing but unclear. As mentioned, inflammation and VEGF induction are known to play important roles in the pathogenesis of AMD.[33,34] Cholesterol and other lipids are known to accumulate in Bruch's membrane and in the choriocapillaris as a process of aging,[73] and 7KCh accumulation has been found at these locations.[8] Moreover, lipoprotein deposits seem to be able to accumulate micromolar levels of 7KCh.[12,13,70] This information, when taken in combination with our data, suggests that 7KCh could potentially play a role in the pathogenesis of AMD. However, until more detailed experiments can be performed in vivo, the role of 7KCh in this process remains hypothetical.

Acknowledgments

The authors thank Robert N. Fariss and Maria M. Campos for their help with HuR protein immunohistochemistry.

References

1. Lordan S, Mackrill JJ, O'Brien NM. Oxysterols and mechanisms of apoptotic signaling: implications in the pathology of degenerative diseases. *J Nutr Biochem.* 2009;20:321–336.
2. Poli G, Sottero B, Gargiulo S, Leonarduzzi G. Cholesterol oxidation products in the vascular remodeling due to atherosclerosis. *Mol Aspects Med.* 2009;30:180–189.
3. Vejux A, Lizard G. Cytotoxic effects of oxysterols associated with human diseases: induction of cell death (apoptosis and/or oncosis), oxidative and inflammatory activities, and phospholipidosis. *Mol Aspects Med.* 2009;30:153–170.

4. Torocsik D, Szanto A, Nagy L. Oxysterol signaling links cholesterol metabolism and inflammation via the liver X receptor in macrophages. *Mol Aspects Med.* 2009;30:134–152.
5. Bjorkhem I, Cedazo-Minguez A, Leoni V, Meaney S. Oxysterols and neurodegenerative diseases. *Mol Aspects Med.* 2009;30:171–179.
6. Olkkonen VM, Hynynen R. Interactions of oxysterols with membranes and proteins. *Mol Aspects Med.* 2009;30:123–133.
7. Brown AJ, Jessup W. Oxysterols: sources, cellular storage and metabolism, and new insights into their roles in cholesterol homeostasis. *Mol Aspects Med.* 2009;30:111–122.
8. Moreira EF, Larrayoz IM, Lee JW, Rodriguez IR. 7-Ketocholesterol is present in lipid deposits in the primate retina: potential implication in the induction of VEGF and CNV formation. *Invest Ophthalmol Vis Sci.* 2009;50:523–532.
9. Smith LL, Teng JI, Kulig MJ, Hill FL. Sterol metabolism, XXIII: cholesterol oxidation by radiation-induced processes. *J Org Chem.* 1973;38:1763–1765.
10. Korytowski W, Bachowski GJ, Girotti AW. Photoperoxidation of cholesterol in homogeneous solution, isolated membranes, and cells: comparison of the 5 alpha- and 6 beta-hydroperoxides as indicators of singlet oxygen intermediacy. *Photochem Photobiol.* 1992;56:1–8.
11. Smith LL. Review of progress in sterol oxidations: 1987–1995. *Lipids.* 1996;31:453–487.
12. Brown AJ, Dean RT, Jessup W. Free and esterified oxysterol: formation during copper-oxidation of low density lipoprotein and uptake by macrophages. *J Lipid Res.* 1996;37:320–335.
13. van Reyk DM, Brown AJ, Hult'en LM, Dean RT, Jessup W. Oxysterols in biological systems: sources, metabolism and pathophysiological relevance. *Redox Rep.* 2006;11:255–262.
14. Rodriguez IR, Fliesler SJ. Photodamage generates 7-keto- and 7-hydroxycholesterol in the rat retina via a free radical-mediated mechanism. *Photochem Photobiol.* 2009;85:1116–1125.
15. Dulak J, Jozkowicz A, Dichtl W, et al. Vascular endothelial growth factor synthesis in vascular smooth muscle cells is enhanced by 7-ketocholesterol and lysophosphatidylcholine independently of their effect on nitric oxide generation. *Atherosclerosis.* 2001;159:325–332.
16. Lemaire S, Lizard G, Monier S, et al. Different patterns of IL-1beta secretion, adhesion molecule expression and apoptosis induction in human endothelial cells treated with 7alpha-, 7beta-hydroxycholesterol, or 7-ketocholesterol. *FEBS Lett letters.* 1998;440:434–439.
17. Prunet C, Lemaire-Ewing S, Menetrier F, Neel D, Lizard G. Activation of caspase-3-dependent and -independent pathways during 7-ketocholesterol- and 7beta-hydroxycholesterol-induced cell death: a morphological and biochemical study. *J Biochem Mol Toxicol.* 2005;19:311–326.
18. Sung SC, Kim K, Lee KA, et al. 7-Ketocholesterol upregulates interleukin-6 via mechanisms that are distinct from those of tumor necrosis factor-alpha, in vascular smooth muscle cells. *J Vasc Res.* 2009;46:36–44.
19. Liu Y, Hulten LM, Wiklund O. Macrophages isolated from human atherosclerotic plaques produce IL-8, and oxysterols may have a regulatory function for IL-8 production. *Arterioscler Thromb Vasc Biol.* 1997;17:317–323.
20. Erridge C, Webb DJ, Spickett CM. Toll-like receptor 4 signalling is neither sufficient nor required for oxidised phospholipid mediated induction of interleukin-8 expression. *Atherosclerosis.* 2007;193:77–85.
21. Joffre C, Leclere L, Buteau B, et al. Oxysterols induced inflammation and oxidation in primary porcine retinal pigment epithelial cells. *Curr Eye Res.* 2007;32:271–280.
22. Lemaire-Ewing S, Berthier A, Royer MC, et al. 7beta-Hydroxycholesterol and 25-hydroxycholesterol-induced interleukin-8 secretion involves a calcium-dependent activation of c-fos via the ERK1/2 signaling pathway in THP-1 cells: oxysterols-induced IL-8 secretion is calcium-dependent. *Cell Biol Toxicol.* 2009;25:127–139.
23. Hakamata H, Miyazaki A, Sakai M, Sakamoto YI, Horiuchi S. Cytotoxic effect of oxidized low density lipoprotein on macrophages. *J Atheroscler Thromb.* 1998;5:66–75.
24. Ramos MA, Kuzuya M, Esaki T, et al. Induction of macrophage VEGF in response to oxidized LDL and VEGF accumulation in human atherosclerotic lesions. *Arterioscler Thromb Vasc Biol.* 1998;18:1188–1196.
25. Inoue M, Itoh H, Tanaka T, et al. Oxidized LDL regulates vascular endothelial growth factor expression in human macrophages and endothelial cells through activation of peroxisome proliferator-activated receptor-gamma. *Arterioscler Thromb Vasc Biol.* 2001;21:560–566.
26. Salomonsson L, Pettersson S, Englund MC, Wiklund O, Ohlsson BG. Post-transcriptional regulation of VEGF expression by oxidised LDL in human macrophages. *Eur J Clin Invest.* 2002;32:767–774.
27. Rodriguez IR, Alam S, Lee JW. Cytotoxicity of oxidized low-density lipoprotein in cultured RPE cells is dependent on the formation of 7-ketocholesterol. *Invest Ophthalmol Vis Sci.* 2004;45:2830–2837.
28. Inoue T, Komoda H, Nonaka M, Kameda M, Uchida T, Node K. Interleukin-8 as an independent predictor of long-term clinical outcome in patients with coronary artery disease. *Int J Cardiol.* 2008;124:319–325.
29. Riazy M, Chen JH, Steinbrecher UP. VEGF secretion by macrophages is stimulated by lipid and protein components of OxLDL via PI3-kinase and PKCzeta activation and is independent of OxLDL uptake. *Atherosclerosis.* 2009;204:47–54.
30. Ghelli A, Porcelli AM, Zanna C, Rugolo M. 7-Ketocholesterol and staurosporine induce opposite changes in intracellular pH, associated with distinct types of cell death in ECV304 cells. *Arch Biochem Biophys.* 2002;402:208–217.
31. Ong JM, Aoki AM, Seigel GM, et al. Oxysterol-induced toxicity in R28 and ARPE-19 cells. *Neurochem Res.* 2003;28:883–891.
32. Dirks WG, MacLeod RA, Drexler HG. ECV304 (endothelial) is really T24 (bladder carcinoma): cell line cross- contamination at source. *In Vitro Cell Dev Biol Anim.* 1999;35:558–559.
33. Morohoshi K, Goodwin AM, Ohbayashi M, Ono SJ. Autoimmunity in retinal degeneration: autoimmune retinopathy and age-related macular degeneration. *J Autoimmun.* 2009;33:247–254.
34. Ozkiris A. Anti-VEGF agents for age-related macular degeneration. *Expert Opin Ther Pat.* 2010;20:103–118.
35. Nabi IR, Mathews AP, Cohen-Gould L, Gundersen D, Rodriguez-Boulan E. Immortalization of polarized rat retinal pigment epithelium. *J Cell Sci.* 1993;104:37–49.
36. Shao R, Guo X. Human microvascular endothelial cells immortalized with human telomerase catalytic protein: a model for the study of in vitro angiogenesis. *Biochem Biophys Res Commun.* 2004;321:788–794.
37. Pedruzzi E, Guichard C, Ollivier V, et al. NAD(P)H oxidase Nox-4 mediates 7-ketocholesterol-induced endoplasmic reticulum stress and apoptosis in human aortic smooth muscle cells. *Mol Cell Biol.* 2004;24:10703–10717.
38. Palozza P, Serini S, Verdecchia S, et al. Redox regulation of 7-ketocholesterol-induced apoptosis by beta-carotene in human macrophages. *Free Radic Biol Med.* 2007;42:1579–1590.
39. Naito Y, Shimozawa M, Manabe H, et al. Azelnidipine, a new calcium channel blocker, inhibits endothelial inflammatory response by reducing intracellular levels of reactive oxygen species. *Eur J Pharmacol.* 2006;546:11–18.
40. Fan XC, Steitz JA. HNS, a nuclear-cytoplasmic shuttling sequence in HuR. *Proc Natl Acad Sci USA.* 1998;95:15293–15298.
41. Doller A, Pfeilschifter J, Eberhardt W. Signalling pathways regulating nucleo-cytoplasmic shuttling of the mRNA-binding protein HuR. *Cell Signal.* 2008;20:2165–2173.
42. Cakir M, Grossman AB. Targeting MAPK (Ras/ERK) and PI3K/Akt pathways in pituitary tumorigenesis. *Expert Opin Ther Targets.* 2009;13:1121–1134.
43. Coulthard LR, White DE, Jones DL, McDermott MF, Burchill SA. p38(MAPK): stress responses from molecular mechanisms to therapeutics. *Trends Mol Med.* 2009;15:369–379.
44. Berthier A, Lemaire-Ewing S, Prunet C, et al. 7-Ketocholesterol-induced apoptosis: involvement of several pro-apoptotic but also anti-apoptotic calcium-dependent transduction pathways. *FEBS Lett J.* 2005;272:3093–3104.
45. Favata MF, Horiuchi KY, Manos EJ, et al. Identification of a novel inhibitor of mitogen-activated protein kinase kinase. *J Biol Chem.* 1998;273:18623–18632.

46. Cuenda A, Rousseau S. p38 MAP-kinases pathway regulation, function and role in human diseases. *Biochem Biophys Acta.* 2007; 1773:1358–1375.
47. Morello F, Perino A, Hirsch E. Phosphoinositide 3-kinase signalling in the vascular system. *Cardiovasc Res.* 2009;82:261–271.
48. Vlahos CJ, Matter WF, Hui KY, Brown RF. A specific inhibitor of phosphatidylinositol 3-kinase, 2-(4-morpholinyl)-8-phenyl-4H-1-benzopyran-4-one (LY294002). *J Biol Chem.* 1994;269:5241–5248.
49. Rask-Madsen C, King GL. Differential regulation of VEGF signaling by PKC-alpha and PKC-epsilon in endothelial cells. *Arterioscler Thromb Vasc Biol.* 2008;28:919–924.
50. Vallabhapurapu S, Karin M. Regulation and function of NF-kappaB transcription factors in the immune system. *Annu Rev Immunol.* 2009;27:693–733.
51. Skaug B, Jiang X, Chen ZJ. The role of ubiquitin in NF-kappaB regulatory pathways. *Annu Rev Biochem.* 2009;78:769–796.
52. Velasco M, Diaz-Guerra MJ, Martin-Sanz P, Alvarez A, Bosca L. Rapid Up-regulation of IkappaBbeta and abrogation of NF-kappaB activity in peritoneal macrophages stimulated with lipopolysaccharide. *J Biol Chem.* 1997;272:23025–23030.
53. Mori N, Yamada Y, Ikeda S, et al. Bay 11–7082 inhibits transcription factor NF-kappaB and induces apoptosis of HTLV-I-infected T-cell lines and primary adult T-cell leukemia cells. *Blood.* 2002; 100:1828–1834.
54. Lizard G, Monier S, Cordelet C, et al. Characterization and comparison of the mode of cell death, apoptosis versus necrosis, induced by 7beta-hydroxycholesterol and 7-ketocholesterol in the cells of the vascular wall. *Arterioscler Thromb Vasc Biol.* 1999; 19:1190–1200.
55. Lizard G, Moisant M, Cordelet C, Monier S, Gambert P, Lagrost L. Induction of similar features of apoptosis in human and bovine vascular endothelial cells treated by 7-ketocholesterol. *J Pathol.* 1997;183:330–338.
56. Chang JY, Liu LZ. Toxicity of cholesterol oxides on cultured neuroretinal cells. *Curr Eye Res.* 1998;17:95–103.
57. Lizard G, Gueldry S, Sordet O, et al. Glutathione is implied in the control of 7-ketocholesterol-induced apoptosis, which is associated with radical oxygen species production. *FASEB J.* 1998;12: 1651–1663.
58. O'Callaghan YC, Woods JA, O'Brien NM. Oxysterol-induced cell death in U937 and HepG2 cells at reduced and normal serum concentrations. *Eur J Nutr.* 1999;38:255–262.
59. Lemaire-Ewing S, Prunet C, Montange T, et al. Comparison of the cytotoxic, pro-oxidant and pro-inflammatory characteristics of different oxysterols. *Cell Biol Toxicol.* 2005;21:97–114.
60. Nishio E, Arimura S, Watanabe Y. Oxidized LDL induces apoptosis in cultured smooth muscle cells: a possible role for 7-ketocholesterol. *Biochem Biophys Res Commun.* 1996;223:413–418.
61. Saito E, Wachi H, Sato F, Seyama Y. 7-Ketocholesterol, a major oxysterol, promotes pi-induced vascular calcification in cultured smooth muscle cells. *J Atheroscler Thromb.* 2008;15:130–137.
62. Leonarduzzi G, Vizio B, Sottero B, et al. Early involvement of ROS overproduction in apoptosis induced by 7-ketocholesterol. *Antioxid Redox Signal.* 2006;8:375–380.
63. Palozza P, Barone E, Mancuso C, Picci N. The protective role of carotenoids against 7-keto-cholesterol formation in solution. *Mol Cell Biochem.* 2008;309:61–68.
64. Galban S, Kuwano Y, Pullmann R Jr, et al. RNA-binding proteins HuR and PTB promote the translation of hypoxia-inducible factor 1alpha. *Mol Cell Biol.* 2008;28:93–107.
65. Koh MY, Powis G. HAF: the new player in oxygen-independent HIF-1alpha degradation. *Cell Cycle.* 2009;8:1359–1366.
66. Moscat J, Rennert P, Diaz-Meco MT. PKCzeta at the crossroad of NF-kappaB and Jak1/Stat6 signaling pathways. *Cell Death Differ.* 2006;13:702–711.
67. Richardson JA, Amantea CM, Kianmahd B, et al. Oxysterol-induced osteoblastic differentiation of pluripotent mesenchymal cells is mediated through a PKC- and PKA-dependent pathway. *J Cell Biochem.* 2007;100:1131–1145.
68. Brown GE, Stewart MQ, Liu H, Ha VL, Yaffe MB. A novel assay system implicates PtdIns(3,4)P(2), PtdIns(3)P, and PKC delta in intracellular production of reactive oxygen species by the NADPH oxidase. *Mol Cell.* 2003;11:35–47.
69. Suzuma I, Suzuma K, Ueki K, et al. Stretch-induced retinal vascular endothelial growth factor expression is mediated by phosphatidylinositol 3-kinase and protein kinase C (PKC)-zeta but not by stretch-induced ERK1/2, Akt, Ras, or classical/novel PKC pathways. *J Biol Chem.* 2002;277:1047–1057.
70. Brown AJ, Watts GF, Burnett JR, Dean RT, Jessup W. Sterol 27-hydroxylase acts on 7-ketocholesterol in human atherosclerotic lesions and macrophages in culture. *J Biol Chem.* 2000;275: 27627–27633.
71. Phillips JE, Geng YJ, Mason RP. 7-Ketocholesterol forms crystalline domains in model membranes and murine aortic smooth muscle cells. *Atherosclerosis.* 2001;159:125–135.
72. McCourt MP, Ashraf K, Miller R, et al. X-ray crystal structure of cytotoxic oxidized cholesterols: 7-ketocholesterol and 25-hydroxycholesterol. *J Lipid Res.* 1997;38:1014–1021.
73. Curcio CA, Millican CL, Bailey T, Kruth HS. Accumulation of cholesterol with age in human Bruch's membrane. *Invest Ophthalmol Vis Sci.* 2001;42:265–274.